Deforestation in the Special Nature Reserve Gornje Podunavlje: Insights from PlanetScope, Sentinel-2 and Landsat-8 Remote Sensing Data

RATKO R. NIKOLIĆ, Vekom Geo d.o.o, Belgrade
ORCID: 0009-0000-5964-030X

Original scientific paper
UDC: 504.122(497.11)
502.13:550.837.7
DOI: 10.5937/tehnika2503263N

Deforestation is a pressing environmental issue, and assessing forest loss with precision is crucial for effective conservation strategies. This study evaluates forest area loss in the Special Nature Reserve "Gornje Podunavlje" over a seven-year period from July 2017 to July 2024. Utilizing remote sensing data from PlanetScope, Sentinel-2, and Landsat-8 satellites, the study employs the XGBoost machine learning classifier to classify forest cover. Results indicate a consistent decline in forest area across all datasets, with reductions from approximately 43 km² in July 2017 to around 33 km² by July 2024. Despite variations in reported forest area due to differences in spatial resolution-PlanetScope (3 meters), Sentinel-2 (10 meters), and Landsat-8 (30 meters)-the overall trend of forest loss is evident. Landsat-8 consistently reported higher forest area compared to PlanetScope and Sentinel-2, attributed to its coarser resolution which may include more edge effects. The high-resolution PlanetScope data allowed for more precise delineation of forest boundaries, enhancing the accuracy of forest cover assessments.

Key Words: *Drought, Sentinel – 1 SAR, Sentinel – 2 MSI, Random Forest*

1. INTRODUCTION

Forests, as a natural resource and a public good, have always been a crucial factor in societal development, serving as a source of goods, services, and consequently, income. The concept of high conservation value forests contributes to sustainable economic development by acting as a significant natural resource for rural development and providing a foundation for adding value to products in sectors such as wood processing, renewable energy, food production, and tourism [1].

Climate change is one of the greatest challenges humanity faces in modern times. Forests and climate are fundamentally connected: the disappearance or degradation of forests is both a cause and a consequence of climate change. [2].

The principal factor contributing to deforestation is the unsustainable utilization of forest resources, which is often marked by the overexploitation of these vital assets. [3] The predominant use of timber is for cutting practices are routinely employed to facilitate the expansion of agricultural land. Furthermore, illegal logging significantly exacerbates the degradation of forest ecosystems, thereby posing an increased threat to these essential environments on a global scale [4].

As significant climate modifiers, forest ecosystems mitigate the effects of individual or multiple climatic factors. At the same time, forests serve as reliable indicators of climatic conditions.

Through substantial temperature regulation, increased condensation of absolute and relative humidity, retention of atmospheric precipitation, influence on cloud forma-tion, reduction of wind speed and strength, and regulation of air composition and oxygen balance, forests are vital climate-regulating systems. In today's climate fluctuations, they play a crucial role in protecting both micro-and macro-climates on a global scale .

Illegal logging is a major problem due to its widespread nature, leading to the destruction of plant and animal life [5]. Regular forestry activities, such as logging for forest renewal, occur when a forest reaches the end of its life cycle and must be regenerated. It is important to distinguish between deforestation or land-use changes and the natural cycle of forest renewal through regular forestry management.

Author's Address: Ratko Nikolić, Vekom Geo d.o.o, Belgrade, Todora Dukina 61
e-mail: ratko.nikolic@vekom.com
Paper received: 16.09.2024
Paper accepted: 31.12.2024.

This research paper will concentrate on the assessment of deforestation within the Special Reserve Gornje Podunavlje, a protected region distinguished by its rich biodiversity and significant forest ecosystems. To facilitate this analysis, Remote Sensing data will be employed from the PlanetScope, Sentinel-2, and Landsat-8 satellites, in conjunction with XGBoost machine learning classifiers, to detect and scrutinize changes in forest cover over time. The temporal scope of the study will encompass the period from July 2017 to July 2024, with the objective of identifying and quantifying deforestation patterns while evaluating the effectiveness of existing conservation strategies. By utilizing these sophisticated technologies, this research aims to deepen the understanding of forest dynamics and to promote more effective management approaches for areas of high conservation value.

2. MATERIALS AND METHODS

2.1. Study Area

The Special Nature Reserve „Gornje Podunavlje“ is located in the peripheral, northwestern regions of Vojvodina. It extends along the left bank of the Danube River and encompasses various ecosystems including meanders, backwaters, channels, as well as aquatic, marshy, meadow, and forest ecosystems formed by the continuous influence of the river (Figure 1).

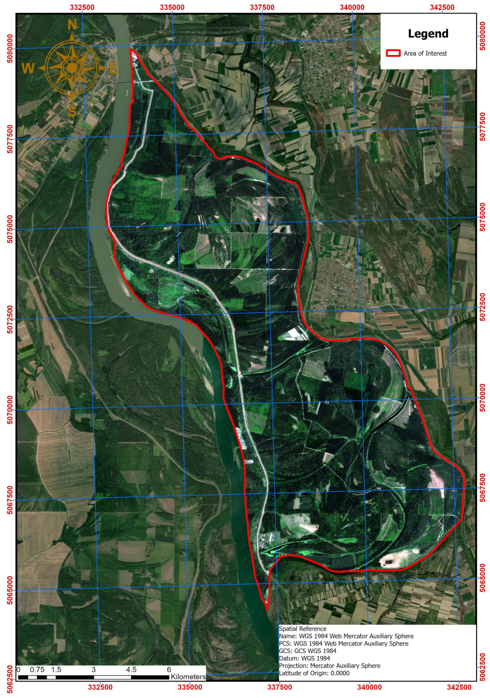

Figure 1 - Study Area (RGB PlanetScope Composite – July 2024)

The Special Nature Reserve „Gornje Podunavlje“ has an irregular and elongated shape. Its northern boundary coincides with the state border between the Republic of Serbia and Hungary. The western boundary is defined by the „main channel of the Danube“, which also represents, as of now, the inter-state, yet to be defined, border between the Republic of Serbia and Croatia. The southern boundary is along the Danube River, which flows west-east after the confluence with the Drava River. The southeastern boundary reaches the border between the municipalities of Apatin and Odžaci, near the bridge between Bogojevo (Republic of Serbia) and Erdut (Croatia).

2.2. Remote Sensing Data

For this study, two free satellite missions were used: Landsat 8 and Sentinel-2, along with PlanetScope commercial data.

Landsat 8, launched in 2013, features the Operational Land Imager (OLI) and Thermal Infrared Sensor (TIRS). It has a temporal resolution of 16 days and a scene width of 185 km. OLI captures nine spectral bands with a spatial resolution of 30 m, while TIRS collects thermal infrared data at 100 m resolution [6].Table 1 outlines the essential characteristics of the Landsat-8 scenes employed in this research, providing information including the Acquisition Date, WRS Path, and WRS Row for each scene. Although these attributes differ among scenes, certain parameters are consistent across all Landsat-8 data utilized. These consistent parameters include the Collection Category (T1), Collection Number (2), Data Type (OLI_TIRS_L1TP), and Sensor Identifier (OLI_TIRS).

Table 1. Attributes of Landsat-8 Scenes Used in the Study

Acquistion Date	WRS Path	WRS Row
2017-07-10	187	029
2018-07-29	187	028
2019-07-07	188	028
2020-07-09	188	028
2021-07-28	188	028
2022-07-15	188	026
2023-07-11	187	028
2024-07-13	187	028

Sentinel-2, part of the ESA's Copernicus program, has a multispectral sensor with 13 bands in visible, NIR, and SWIR regions [7]. It has a spatial resolution of 10, 20, and 60 m, a temporal resolution of 5 days, and a scene width of 290 km. Data were obtained via Copernicus Open Access Hub (https://-scihub.-copernicus.eu/, accessed on 14 August 2024).

Table 2 provides key attributes of the Sentinel-2 scenes used in the research, detailing the Mission ID, Acquisition Date, Processing Baseline Number, and Tile ID for each scene. These specific attributes vary for each scene, while other information remains consistent across all the Sentinel-2 data used. For example, all scenes were processed to Level-2A, with the product type classified as S2MSI2A, and captured during a descending orbit.

Table 2. Attributes of Sentinel-2 Scenes Used in the Study

Mission ID	Acquistion Date	Processing Baseline Number	Tile ID
S2B	2017-07-19	N0500	T34TCR
S2B	2018-07-14	N0208	T33TYL
S2B	2019-07-19	N0500	T34TCR
S2A	2020-07-28	N0500	T34TCR
S2A	2021-07-13	N0500	T34TCT
S2A	2022-07-23	N0400	T34TCR
S2A	2023-07-13	N0509	T34TCR
S2A	2024-07-30	N0511	T33TYL

PlanetScope is a satellite imaging constellation managed by Planet Labs, providing high-resolution data with a spatial resolution of approximately 3 meters. The system comprises a substantial fleet of small, lightweight satellites, referred to as "Doves," facilitating daily global coverage. This frequent data acquisition is crucial for monitoring rapid environmental changes, including deforestation and agricultural trends. PlanetScope captures imagery across four spectral bands: red, green, blue, and near-infrared, which enhances its applicability for various remote sensing tasks.

Table 3 provides unique attributes of the PlanetScope scenes used in the research, including Acquisition Date, Instrument, Satellite ID, and Strip ID for each scene. While these attributes differ across the dataset, several parameters are consistent across all PlanetScope scenes. These include the acquisition type (NOMINAL), product type (L3B), status (ARCHIVED), orbit type (LEO-SSO), sensor type (OPTICAL), and spatial resolution of 3 meters.

Table 3. Attributes of Landsat-8 Scenes Used in the Study

Acquistion Date	Instrument	Satellite ID	Strip ID
2017-07-30	PS2	1032	656029
2018-07-30	PS2	1024	1600606
2019-07-21	PS2	0f12	2537742
2020-07-29	PSB.SD	220b	3608098
2021-07-28	PSB.SD	2441	4737910
2022-07-29	PSB.SD	2457	5819244
2023-07-31	PSB.SD	249c	6683555
2024-07-30	PSB.SD	24c0	7475166

2.3 Vegetation Indices

In this study, several spectral indices were calculated to assess vegetation characteristics and enhance the classification between Forest and Non-Forest areas. These indices utilized various combinations of near-infrared, red, and green reflectances to provide insights into vegetation health, cover, and soil influence. The specific indices used are detailed in Table 4, which summarizes their application and relevance to the analysis.

Table 4. Spectral Indices

Spectral Index	Cal. Formula	Ref.
NDVI	$\frac{\rho_{nir} - \rho_{red}}{\rho_{nir} + \rho_{red}}$	[8]
GNDVI	$\frac{\rho_{nir} - \rho_{green}}{\rho_{nir} + \rho_{green}}$	[9]
RVI	$\frac{\rho_{nir}}{\rho_{red}}$	[10]
SAVI	$\frac{(\rho_{nir} - \rho_{red}) \times (1 + L)}{\rho_{nir} + \rho_{red} + L}$	[11]
MSAVI	$\frac{(1 + M) \times (\rho_{nir} - \rho_{red})}{\rho_{nir} + \rho_{red} + L}$	[12]
DVI	$\rho_{nir} - \rho_{red}$	[13]
IPVI	$\frac{\rho_{nir} - \rho_{red}}{\rho_{red}}$	[14]
BI	$\rho_{red} + \rho_{swir1} - \rho_{nir}$	[15]
BSI	$\frac{\rho_{swir2} + \rho_{red} - \rho_{nir} - \rho_{blue}}{\rho_{swir2} + \rho_{red} + \rho_{nir} + \rho_{blue}}$	[16]
NBR	$\frac{\rho_{nir} - \rho_{swir2}}{\rho_{nir} + \rho_{swir2}}$	[17]
DBSI	$\frac{\rho_{swir2} - \rho_{green}}{\rho_{swir2} + \rho_{green}} - NDVI$	[18]

2.4 Training and Validation Data

The training and validation data for the classification models were derived from PlanetScope RGB composite imagery. Two classes were defined: Forest and Non-Forest. Data points for both training and validation were created using visual inspection, ensuring that selected points consistently represented forested or non-forested areas throughout the entire study period (2017–2024).

For training, approximately 216,000 data points were carefully selected and validated across multiple years to confirm their consistency. This approach minimized the risk of misclassification caused by temporary land cover changes or seasonal variations. For validation, 175,000 data points were designated, ensuring that the dataset was sufficiently large and diverse to accurately evaluate the models' performance.

2.4 Classification Approach

In this study, the Gradient Boosting algorithm (*XGBoost*) [19][1] was applied to classify Forest and Non-Forest areas using remote sensing data from Sentinel-2, Landsat-8, and Planet Scope. Gradient Boosting, a robust ensemble machine learning technique, builds models incrementally by combining the outputs of weaker learners to improve overall accuracy.

In the context of accuracy, gradient boosting methods are recognized as among the most effective techniques within the realms of boosting and machine learning as a whole. Furthermore, the training process associated with these methods can be regarded as relatively efficient. [20][20]

The fundamental concept originates from gradient optimization methods, which focus on enhancing the existing solution to an optimization problem by incorporating a vector that is proportional to the negative gradient of the function that is being minimized.

2.5 Classification Accuracy Assessment

To assess the accuracy of the model classification, several quantitative measures were utilized, derived from predictions on test data and generated using a confusion matrix [21]

Table 5 describes the typical structure of a confusion matrix for binary classification. The confusion matrix provides a detailed breakdown of the classification performance by presenting the counts of true positives (TP), false positives (FP), true negatives (TN), and false negatives (TN).

Table 5. Matrix confusion for binary classification

		Reference	
		Positive	Negative
Prediction	Positive	tp	fp
	Positive	fn	tn

Table 6 shows the measures used to evaluate classification accuracy along with their formulas.

Table 6. Measure for binary classification

Measure	Formula	
Overall Accuracy	$\frac{tp+tn}{tp+fn+fp+tn}$	(1)
PA of the Forest class	$\frac{tp}{tp+fn}$	(2)
PA of the Non-Forest class	$\frac{tn}{tn+fp}$	(3)
UA of the Forest class	$\frac{tp}{tp+fp}$	(4)
UA of the Non-Forest class	$\frac{tn}{tn+fn}$	(5)

These measures are derived from the confusion matrix and include Overall Accuracy, Producer (PA) and User's Accuracy (UA) and kappa koef. Each measure is calculated based on the counts of true positives, false negatives, false positives, and true negatives presented in the confusion matrix.

In this study, Cohen's kappa was used as a metric to evaluate the accuracy of classification results. The kappa statistic is calculated using the formula [22]:

$$k = \frac{Pr(a)-Pr\,(e)}{1-Pr\,(e)} \qquad (5)$$

where $Pr\ (a)$ represents the actual observed agreement between classifications, and $Pr\ (e)$ represents the expected agreement by chance. This metric provided a measure of how well the classification results aligned with actual observations, accounting for chance agreement.

3. RESULTS

3.1 Forest Loss

This chapter details the findings from an analysis of forest area loss utilizing classification with the XGBoost algorithm and remote sensing data from PlanetScope, Sentinel-2, and Landsat-8.

The Figure 2. illustrates the changes in forest area over time from July 2017 to July 2024, using three different remote sensing datasets: PlanetScope, Sentinel-2, and Landsat-8. Each dataset provides valuable insights into forest cover dynamics, showcasing trends and variations across the years.

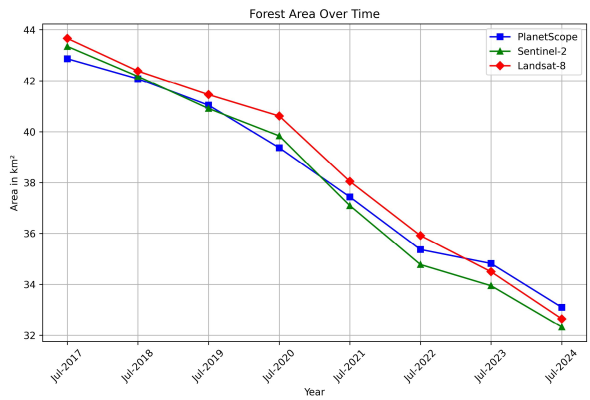

Figure 2 - Temporal Changes in Forest Area (Jul 2017 - Jul 2024)

Starting with the values from July 2017, the forest area observed by Planet Scope was approximately 42.86 km², Sentinel-2 recorded 43.35 km², and Landsat-8 noted 43.66 km². Over the following years, all three datasets indicate a consistent decrease in forest area, reflecting a notable trend of forest loss. By July 2024, the forest area had declined to around 33.09 km² according to Planet Scope, 32.29 km² as per Sentinel-2, and 32.64 km² according to Landsat-8. This reduction demonstrates a significant decrease in forest coverage, with Planet Scope and Sentinel-2 showing a somewhat similar rate of decline, while Landsat-8 provides slightly higher values across the same period.

Among the datasets, Landsat-8 consistently reported the highest forest area throughout the study period, whereas Planet Scope and Sentinel-2 showed lower but relatively comparable values. The differences in reported areas can be attributed to variations in spatial resolution and sensor characteristics among the remote sensing platforms. The uniform trend across all datasets highlights a genuine reduction in forest cover rather than discrepancies caused by data inconsistencies.

Table 7. Annual Forest Loss by Remote Sensing Data

	Annual Forest Loss		
Period	Planet Scope [km^2]	Sentinel -2 [km^2]	Landsat-8 [km^2]
2017-2018	0.79	1.18	1.29
2018-2019	1.03	1.27	0.92
2019-2020	1.67	1.07	0.84
2020-2021	1.94	2.74	2.57
2021-2022	2.07	2.32	2.14
2022-2023	0.55	0.83	1.41
2023-2024	1.72	1.62	1.85

The Table 7. presents the annual forest loss (in km²) for each period between 2017 and 2024, as observed by three different remote sensing platforms: Planet Scope, Sentinel-2, and Landsat-8.

From 2017 to 2018, Sentinel-2 recorded the highest forest loss at 1.18 km², while Planet Scope measured 0.79 km², and Landsat-8 reported 1.29 km². Over the next two years, from 2018 to 2020, the data shows a general trend of declining forest loss, with Planet Scope indicating a loss of 1.03 km² and 1.67 km², respectively. Notably, the period between 2020 and 2021 saw the highest loss for all three datasets, with Sentinel-2 recording a peak loss of 2.74 km² and Landsat-8 at 2.57 km², while Planet Scope showed 1.94 km².

Between 2021 and 2024, the loss values fluctuated. From 2021 to 2022, the forest loss remained relatively high, with PlanetScope measuring 2.07 km², Sentinel-2 recording 2.32 km², and Landsat-8 showing 2.14 km². However, from 2022 to 2023, the loss values significantly dropped, particularly for PlanetScope (0.55 km²). In the final period from 2023 to 2024, all datasets again recorded increased forest loss, with Landsat-8 showing the highest value at 1.85 km², followed closely by PlanetScope at 1.72 km² and Sentinel-2 at 1.62 km².

Figure 3 - RGB Composites of Forest Area for July 2017

Figure 4 - Classification Maps of Forest and Non-Forest Areas Derived from PlanetScope(left), Sentinel-2 (middle) and Landsat-8 (right) Data July 2017

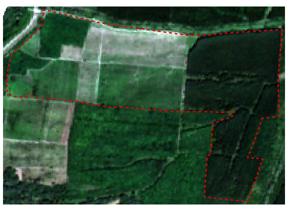

Figure 5 - RGB Composites of Forest Area for July 2020

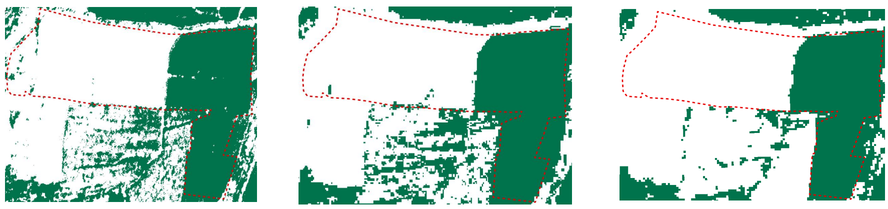

Figure 6 - Classification Maps of Forest and Non-Forest Areas Derived from PlanetScope(left), Sentinel-2 (middle) and Landsat-8 (right) Data July 2020

Figure 7 - RGB Composites of Forest Area for July 2024

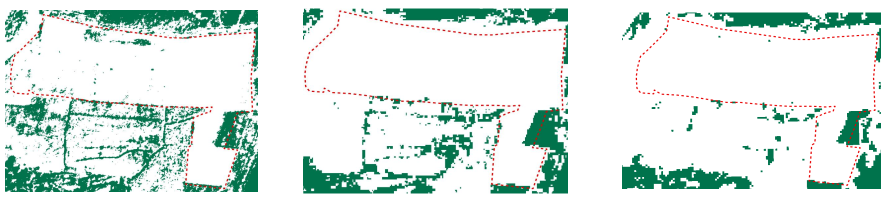

Figure 8 - Classification Maps of Forest and Non-Forest Areas Derived from PlanetScope(left), Sentinel-2 (middle) and Landsat-8 (right) Data July 2024

Figures 3, 5, and 7 provide examples of the progression of deforestation in the study area over time. Figure 3 shows an RGB PlanetScope composite of the forest area from July 2017. The red dashed line marks the forest extent at the beginning of the study, covering an area of 1.27 km². Figure 5 presents the same area from July 2020, showing the impact of deforestation. By this time, approximately 0.7 km2 of the original forest had been lost, highlighting significant deforestation.

Figure 7 depicts the RGB PlanetScope composite from July 2024, indicating that the forest cover has completely disappeared from the study area, reflecting continued deforestation over the observed period. Figures 4, 6, and 8 provide classification maps derived from PlanetScope (left), Sentinel-2 (middle), and Landsat-8 (right) data for July 2017, 2020, and 2024, respectively. These maps reveal the spatial distribution of forest and non-forest areas, showcasing how different satellite sensors have captured the transformation of the landscape over time. The classification maps offer a comparative view of the effectiveness of each sensor in detecting changes in land cover and illustrate the extent of deforestation.

3.2 Model Training Results

This section presents essential metrics for evaluating classification accuracy, namely OA, the Kappa statistic, PA and UA. OA serves as a broad indicator of performance, whereas the Kappa statistic adjusts for chance agreement, yielding a more accurate evaluation. UA assesses the correctness of classified instances, while PA measures the proportion of accurately identified true instances.

The Kappa values shown in Figure 9. represent the performance of classification models from PlanetScope, Sentinel-2, and Landsat-8 over several years, measured by the Kappa statistic. This metric evaluates the agreement between classified data and ground truth, adjusting for the possibility of chance agreement.

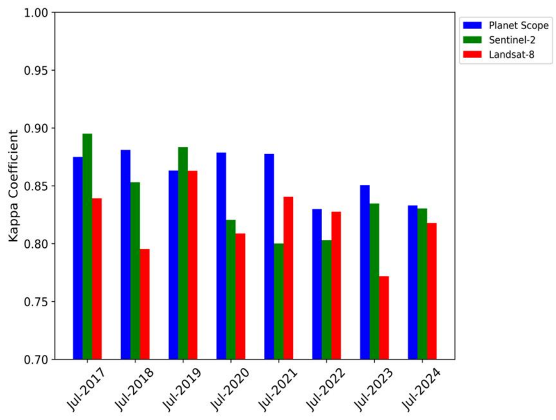

Figure 9 - Kappa coef. of Classification Models

Planet Scope demonstrates relatively stable Kappa values, ranging from 0.83 to 0.88. The highest Kappa value is recorded in July 2018 at 0.88, indicating a high level of agreement with ground truth. The lowest Kappa value, 0.83, is observed in July 2022 and 2024, suggesting slightly lower but still considerable agreement.

Sentinel-2 shows more variation in Kappa values, ranging from 0.80 to 0.90. The highest Kappa value, 0.90, is noted in July 2017, reflecting the highest agreement with ground truth among the three platforms.

Landsat-8 presents Kappa values ranging from 0.77 to 0.86. The highest Kappa value, 0.86, is recorded in July 2019, suggesting a strong agreement with ground truth. The lowest Kappa value of 0.77 is observed in July 2022, similar to Sentinel-2's lowest value, indicating the least agreement in that year.

Overall, the Kappa values for all three platforms indicate generally high agreement with ground truth, with Sentinel-2 achieving the highest Kappa value in July 2017, showing the best performance in terms of accuracy adjustment.

PlanetScope and Landsat-8 also exhibit strong performance, though with some variation across different years. These results reflect the effectiveness of each platform in accurately classifying data while accounting for chance agreement.

Figure 10 displays the PA and UA for the Forest and Non-Forest classes specifically for Planet Scope over several years.

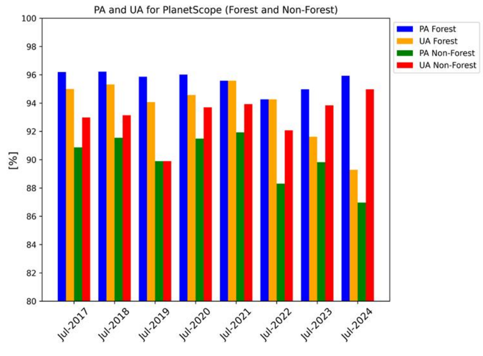

Figure 10 - Producer's and User's Accuracy for Forest and Non-Forest Classes - PlanetScope Data

For the Forest class, PA ranges from 94.26% to 96.22%, reflecting consistently high accuracy in identifying true forest areas, with the peak performance in July 2018. The UA for the Forest class ranges from 89.28% to 95.58%, with the highest accuracy also recorded in July 2021, although it decreases to 89.28% in July 2024, indicating a slight reduction in classification confidence.

For the Non-Forest class, PA ranges from 86.97% to 91.93%, demonstrating strong performance in detecting non-forest areas, with the highest accuracy observed in July 2021. The UA for Non-Forest ranges from 89.90% to 94.97%, with the highest confidence noted in July 2024, suggesting effective classification of non-forest regions.

Figure 11. illustrates the PA and UA for the Forest and Non-Forest classes using Sentinel-2 data.

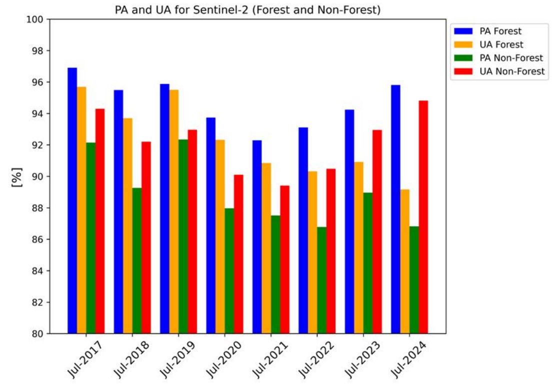

Figure 11 - Producer's and User's Accuracy for Forest and Non-Forest Classes – Sentinel-2 Data

For the Forest class, the PA ranges from 92.29% to 96.91%, demonstrating Sentinel-2's reliable performance in identifying forested regions, with the highest accuracy recorded in July 2017. The UA for the Forest class spans from 89.17% to 95.70%, also peaking in July 2017. However, a decline in UA to 89.17% was noted in July 2024, suggesting a reduction in classification confidence.

In the case of the Non-Forest class, PA values range from 86.78% to 92.34%, indicating robust performance in detecting non-forest areas, with the maximum PA achieved in July 2019. The UA for the Non-Forest class varies from 89.41% to 94.82%, with the highest confidence noted in July 2024; however, a significant decrease to 89.41% was observed in July 2021.

Figure 12. displays the PA and UA for the Forest and Non-Forest classes derived from Landsat-8 data.

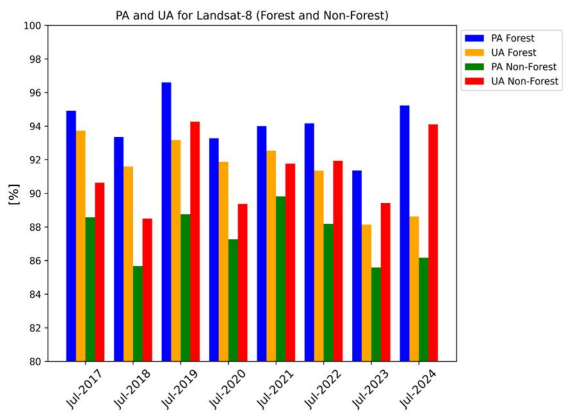

Figure 12 - Producer's and User's Accuracy for Forest and Non-Forest Classes – Landsat-8 Data

For the Forest class, PA ranges from 91.36% to 96.61%, with peak accuracy in July 2019, and UA ranges from 88.14% to 93.73%, reaching its highest in July 2017. For the Non-Forest class, PA varies between 85.59% and 89.82%, with the highest PA in July 2021, and UA ranges from 88.50% to 94.27%, peaking in July 2021. Overall, Landsat-8 shows strong performance with high accuracy for both classes, especially in July 2019.

4. DISCUSSION

The analysis of forest area loss over the period from July 2017 to July 2024, using remote sensing data from PlanetScope, Sentinel-2, and Landsat-8, reveals significant insights into forest cover dynamics. All three datasets consistently indicate a decline in forest area, underscoring a persistent trend of forest loss. Despite the variations in reported forest area between the datasets, the overall trend is clear: a substantial reduction in forest cover over the study period.

The data highlights a consistent decrease in forest area across all platforms. PlanetScope, Sentinel-2, and Landsat-8 all show a decline from approximately 43 km² in July 2017 to around 33 km² by July 2024. While Landsat-8 consistently reported higher forest area, the overall trend of decline is consistent across the datasets. This agreement supports the robustness of the observed forest loss trend, suggesting that it is a genuine phenomenon rather than a result of data discrepancies.In analyzing why Landsat-8 consistently reported higher forest area compared to Planet Scope and Sentinel-2, one key factor is its spatial resolution. Landsat-8 has a spatial resolution of 30 meters, which, while coarser than the 3 meters of Planet Scope and Sentinel-2's 10 meters, can still impact classification results significantly. The larger pixel size of Landsat-8 can include more edge effects, where pixels at the boundary between forest and non-forest areas might still be classified as forest due to partial coverage by trees. This phenomenon is particularly relevant in areas with mixed land cover or where forest edges are not sharply defined.

Given Planet Scope's high spatial resolution of 3 meters, it can capture detailed forest boundaries and finer spatial features. This resolution might allow for more precise delineation of forested areas, leading to potentially smaller or more accurate measurements of forest cover compared to sensors with coarser resolutions.

An essential aspect to consider is the influence of spectral resolution on the measurement of forest areas. The three satellite missions utilized in this study—PlanetScope, Sentinel-2, and Landsat-8—exhibit distinct spectral capabilities. PlanetScope is characterized by limited spectral coverage, primarily targeting visible and near-infrared (NIR) bands, while Sentinel-2 and Landsat-8 incorporate additional spectral bands, including Shortwave Infrared (SWIR). These SWIR bands are particularly effective in assessing vegetation properties and forest conditions. Consequently, it is crucial to evaluate whether the analysis employed all available spectral bands or if it was confined to the common bands shared among the sensors.

Should the analysis have relied solely on the common bands, there may have been a significant loss of valuable spectral information, especially from Sentinel-2 and Landsat-8, which are equipped with bands that excel in vegetation monitoring. For example, the SWIR bands enhance the ability to detect forest degradation, assess soil moisture, and identify subtle signs of vegetation stress—elements that may not be adequately captured by PlanetScope.

In this study, spectral indices that incorporate SWIR bands, particularly those derived from Sentinel-2 and Landsat-8, were employed to enhance the accuracy of forest area classification. These indices offered improved sensitivity to vegetation dynamics, which is vital for effective forest monitoring.

The lack of SWIR bands in PlanetScope data may have impacted its reported forest areas, particularly in regions where SWIR-sensitive indices could identify changes that are not detectable through NIR and visible bands. Future analyses should thoughtfully weigh the trade-offs between standardizing spectral inputs and utilizing the full spectral capabilities of each sensor, aiming for a balanced and comprehensive evaluation.

5. CONCLUSIONS

The analysis of forest area loss from July 2017 to July 2024, utilizing remote sensing data from PlanetScope, Sentinel-2, and Landsat-8, underscores a significant and consistent decline in forest cover within the Special Nature Reserve „Gornje Podunavlje“. All three datasets, despite their differences in spatial resolution, reveal a clear and persistent trend of forest loss over the study period.

Initially, in July 2017, the forest area was approximately 43 km² across the datasets, but by July 2024, it had decreased to around 33 km². This reduction is evident in all three datasets, supporting the robustness of the observed trend and indicating a genuine decrease in forest cover. The agreement across PlanetScope, Sentinel-2, and Landsat-8 emphasizes the reliability of the forest loss trend, notwithstanding variations in reported forest area due to differences in spatial resolution. Landsat-8 consistently reported higher forest area compared to PlanetScope and Sentinel-2. This discrepancy can be attributed to Landsat-8's coarser spatial resolution of 30 meters, which may result in more edge effects and mixed land cover pixels being classified as forest. In contrast, PlanetScope's higher resolution of 3 meters allows for more precise delineation of forest boundaries, potentially leading to more accurate measurements of forest cover.

Despite these differences in spatial resolution, the overall trend of forest loss is consistently captured across all datasets. This multi-sensor approach reinforces the validity of the observed deforestation and highlights the importance of considering spatial resolution when interpreting remote sensing data. The findings underscore the need for continued monitoring and targeted conservation efforts to address and mitigate the impacts of forest loss in the region.

This study took into account the spectral resolution of various satellites, utilizing vegetation-sensitive spectral indices that incorporate Shortwave Infrared (SWIR) bands wherever they are available, as detailed in Table 4. The integration of these SWIR bands, especially from Sentinel-2 and Landsat-8, significantly improved the analysis by enhancing the detection of vegetation conditions and forest cover. Conversely, the limited spectral coverage of PlanetScope, which does not include SWIR bands, may lead to inconsistencies in forest area measurements when compared with Sentinel-2 and Landsat-8.

Despite the differences in spatial and spectral resolution, the trend of forest loss observed remains consistent and robust across all datasets. This consistent trend emphasizes the critical importance of employing multi-sensor approaches in studies focused on deforestation, allowing for a comprehensive understanding that leverages the strengths while addressing the limitations of various satellite missions.

The results of this study underscore the pressing need for continuous monitoring and the imple-mentation of targeted conservation strategies to combat the significant forest loss in Gornje Podunavlje. Future research endeavors should consider the incorporation of additional spectral information and advanced vegetation indices, which could greatly enhance the accuracy of forest cover assessments.

6. ACKNOWLEDGMENTS

I would like to express my sincere gratitude to company Vekom Geo d.o.o. for providing PlanetScope satellite imagery, which was crucial for the successful completion of this research.

REFERENCES

[1] Baldrian P. Forest microbiome: diversity, complexity and dynamics. *FEMS microbiology reviews*, 41 2, 109-130. https://doi.org/10.1093/femsre/fuw040, 2016.

[2] Bonan G. Forests and Climate Change: Forcings, Feedbacks, and the Climate Benefits of Forests. *Science*, 320, 1444 - 1449. https://-doi.org/-10.1126/-science.1155121, 2008.

[3] Busch J. & Ferretti-Gallon K. What Drives Deforestation and What Stops It? A Meta-Analysis. *Review of Environmental Economics and Policy*, 11, 3 - 23. https://doi.org/10.1093/reep/rew013, 2017.

[4] Thompson S. & Magrath W. Preventing illegal logging. *Forest Policy and Economics*. https://-doi.org/10.1016/J.FORPOL.2021.102479, 2021.

[5] Reboredo, F. Socio-economic, environmental, and governance impacts of illegal logging. *Environment Systems and Decisions*, 33, 295-304. https://-doi.org/10.1007/s10669-013-9444-7, 2013.

[6] Storey J, Choate M, Lee K, Landsat 8 Operational Land Imager On-Orbit Geometric Calibration and Performance. *Remote Sens.* 6, 11127-11152. https://-doi.org/10.3390/rs61111127, 2014.

[7] Copernicus Sentinel-2 (processed by ESA), 2021, MSI Level-2A BOA Reflectance Product. Collection 1. European Space Agency. https://-doi.org/-10.-5270/S2_-znk9xsj, 2021.

[8] Huete A, Didan K, Miura T, Rodriguez E. P, Gao, X., & Ferreira, L. G. Overview of the radiometric and biophysical performance of the MODIS vegetation indices. *Remote sensing of environment*, 83(1-2), 195-213, 2002.

[9] Rahman M. & Robson A. Integrating Landsat-8 and Sentinel-2 Time Series Data for Yield Prediction of Sugarcane Crops at the Block Level. *Remote. Sens*, 12, 1313. https://doi.org/10.3390/rs12081313, 2020.

[10] Gupta R. K. Comparative study of AVHRR ratio vegetation index and normalized difference vegeta-tion index in district level agricultural monitoring. *International Journal of Remote Sensing*, 14(1), 53–73. https://doi.org/10.1080/01431169308904321, 1993.

[11] Huete, A. R. A soil-adjusted vegetation index (SAVI). *Remote Sensing of Environment*, 25(3), 295–309. https://doi.org/10.1016/0034-4257(88)90106-X, 1988.

[12] Qi J, Chehbouni A, Huete A. R, Kerr Y. H. & Sorooshian S. A modified soil adjusted vegetation index. *Remote Sensing of Environment*, 48(2), 119–126. https://doi.org/10.1016/0034-4257(94)90134-1, 1994.

[13] Sousa D, Small C. Which Vegetation Index? Benchmarking Multispectral Metrics to Hyperspectral Mixture Models in Diverse Cropland. *Remote Sensing*. 15(4):971. https://doi.org/-10.3390/-rs-150-40971, 2023.

[14] Crippen R. E. Calculating the vegetation index faster. *Remote Sensing of Environment*, 34(1), 71–73. https://doi.org/10.1016/0034-4257(90)90085-Z, 1990.

[15] Lin H, Wang J, Liu S, Qu Y. & Wan H. Studies on urban areas extraction from landsat TM images. In Proceedings. 2005 *IEEE International Geoscience and Remote Sensing Symposium*, 2005. IGARSS'05. (Vol. 6, pp. 3826-3829). Ieee, 2005.

[16] Diek S, Fornallaz F, Schaepman M. E, De Jong R. Barest Pixel Composite for Agricultural Areas Using Landsat Time Series. *Remote Sens.* 9, 1245. https:-//doi.org/10.3390/rs9121245, 2017.

[17] Alcaras E, Costantino D, Guastaferro F, Parente C, Pepe M. Normalized Burn Ratio Plus (NBR+): A New Index for Sentinel-2 Imagery. *Remote Sens*. 14, 1727. https://doi.org/10.3390/rs14071727, 2022.

[18] Rasul A, Balzter H, Ibrahim G. R. F, Hameed H. M, Wheeler J, Adamu B, Ibrahim S, Najmaddin P. M. Applying Built-Up and Bare-Soil Indices from Landsat 8 to Cities in Dry Climates. Land 2018, 7, 81. https://doi.org/10.3390/land7030081, 2018

[19] Chen T, & Guestrin C, XGBoost: A scalable tree boosting system. Proceedings of the *22nd ACM SIGKDD International Conference on Knowledge Discovery and Data Mining*, 785–794. https://doi.org/10.1145/2939672.2939785, 2016.

[20] Béntéjac C, Csörgő A. & Martínez-Muñoz G. A comparative analysis of gradient boosting algorithms. *Artificial Intelligence Review*, 54(3), 1937–1967. https://doi.org/10.1007/s10462-020-09896-5, 2021.

[21] Nicolau A. P, Dyson K, Saah D, & Clinton N. Accuracy assessment: Quantifying classification quality. In J. A. Cardille, M. A. Crowley, D. Saah, & N. E. Clinton (Eds.), *Cloud-based remote sensing with Google Earth Engine: Fundamentals and applications* (pp. 135–145). Springer International Publishing. https://doi.org/10.1007/978-3-031-26588-4_7, 2024.

[22] Kvålseth, T. Note on Cohen's Kappa. Psychological Reports, 65, 223 - 226. https://-doi.org/-10.2466/-pr0.1989.65.1.223, 1989.

REZIME

DEFORESTACIJA U SPECIJALNOM REZERVATU PRIRODE GORNJE PODUNAVLJE: UVIDI NA OSNOVU PLANETSCOPE, SENTINEL-2 I LANDSAT-8 PODATAKA DALJINSKE DETEKCIJE

Deforestacija je ozbiljan ekološki problem, a precizno procenjivanje gubitka šumskih površina ključno je za efikasne strategije očuvanja. Ova studija procenjuje gubitak šumskih površina u Specijalnom rezervatu prirode „Gornje Podunavlje“ tokom sedmogodišnjeg perioda, od jula 2017. do jula 2024. godine. Koristeći podatke daljinske detekcije satelitskih misija PlanetScope, Sentinel-2 i Landsat-8, u Studiji se primenjuje XGBoost algoritam mašinskog učenja za klasifikaciju šumskog pokrivača. Rezultati pokazuju konzistentan pad šumskih površina u svim skupovima podataka, sa smanjenjem od, približno, 43 km² u julu 2017. na, približno, 33 km² do jula 2024. godine. Iako postoje varijacije u prijavljenim površinama šuma zbog razlika u prostornoj rezoluciji - Planet-Scope (3 metra), Sentinel-2 (10 metara) i Landsat-8 (30 metara) - ukupan trend gubitka šuma je očigledan. Landsat-8 je dosledno prijavljivao veće površine šuma u poređenju sa PlanetScope i Sentinel-2, što se pripisuje njegovoj grubljoj rezoluciji koja može uključiti više ivica šuma. Podaci visoke rezolucije PlanetScope-a omogućili su preciznije razgraničenje šumskih granica, poboljšavajući tačnost procena šumskog pokrivača

Ključne reči: *suša, Sentinel - 1 Radar sa sintetičkom aperturom, Sentinel - 2 multispektralni senzor I XGBoost*